OPTIMIZATION OF VIBRO-ACOUSTIC BY TOOTH HARMONICS OF IPMSM FOR EV UNDER MULTIPLE OPERATING CONDITIONS

Sili Ma[1], Quanfeng Li[2*]

[1]Shanghai DianJi University,Shanghai, China
[2] Shanghai DianJi University,Shanghai, China
**liqf@sdju.edu.cn*

Keywords: VIBRO-ACOUSTIC; SKEWED POLES; TOOTH HARMONICS; ELECTRIC VEHICLES

Abstract

Vibro-acoustic is very important considerations in the design of interior permanent magnet synchronous motor (IPMSM) for electric vehicles (EV). In this paper, the problem of large vibro-acoustic of 8-pole 48-slot IPMSM under multiple operating conditions (MOC) is theoretically analyzed to be caused by the first-order tooth harmonics. Vibro-acoustic reduction effects of continuous segmented skewed poles and V-shape segmented skewed poles are compared by finite element analysis (FEA) and optimization of the rotor with 8-segment V-shape skewed poles is given. Finally, the equivalent radiated power level (ERPL) at the largest vibration order caused by tooth harmonics of the optimized motor is decreased by 14.9%; the A-weighted sound pressure level (SPL) at 3500 RPM and 5500 RPM are decreased by 19.7% and 17.6%, respectively.

1 Introduction

NVH performance is recognized as a primary indicator for assessing the quality and market competitiveness of new energy electric vehicles. The IPMSM is widely used in EV due to its distinct advantages in power factor and efficiency [1]. However, unlike fuel-powered vehicles, new energy electric vehicles are driven by electric motors. Due to the absence of internal combustion engine noise masking effects, the NVH issues of IPMSMs are accentuated [2]. The vibro-acoustic of IPMSM can be categorized into three types according to the source: electromagnetic vibro-acoustic, aerodynamic vibro-acoustic and mechanical vibro-acoustic [3]. Among them, electromagnetic vibration is the main source of motor vibro-acoustic, generated by harmonic EMF excitation, which can act on the stator teeth, leading to structural deformation and inducing motor vibration [4]. Its electromagnetic vibration characteristics are mainly determined by the spatial harmonic properties of the EMF, in which the zero-order radial force wave plays a dominant role in the vibration response [5]. A phase compensation method based on vibrational conductivity theory and operational force measurements can accurately identify the main excitation source under multi-physics field coupling[6].

Skewed slots and skewed poles can effectively reduce tooth harmonics and have a good effect on the electromagnetic vibro-acoustic of the motor [7]. For permanent magnet synchronous motors, the rotor segmented miter method is often used. Compared with the traditional slotted pole method, the rotor segmented pole method is simple and convenient for pole assembly, and can effectively suppress electromagnetic noise [8]. Conventional approaches primarily employed continuous skewed rotors to spatially distribute harmonic fields along the axial direction [9].

In this paper, in order to improve the 8-pole 48-slot IPMSM with high vibro-acoustic due to tooth harmonics, the noise reduction effects of continuous skewed poles and V-skewed poles are compared, and then an optimization scheme of 8-section V-skewed poles is given for the rotor to optimize the harmonic electromagnetic field, the vibration ERPL, and the A-weighted SPL of the motor. Finally, the comprehensive optimization of the NVH performance of the motor under MOC conditions with the proposed optimization scheme is completed by FEA.

2. EMF and Vibro-acoustic Analysis

2.1 EMF analysis

Neglecting the tangential component of the air-gap flux density, the radial EMF wave generated by the harmonic magnetic fields of the stator and rotor, according to the Maxwell tensor method, is expressed as equation (1):

$$p_{v\mu} = \frac{(B_v + B_\mu)^2}{2\mu_0} = \frac{B_v^2 + 2B_vB_\mu + B_\mu^2}{2\mu_0} \tag{1}$$

Where: μ, v are the number of stator and rotor magnetic field harmonics, B_v, B_μ is the stator and rotor radial harmonic flux density, μ_0 is the vacuum permeability.

From equation (1), it can be seen that the radial EMF wave component is mainly composed of three parts, the first and third items are generated by the stator and rotor magnetic fields alone, and the second item is generated by the stator and rotor magnetic fields together. Since the force wave generated by BB is of higher order, and the stator surface deformation displacement amplitude is inversely proportional to the fourth power of the EMF wave order, their impact on vibro-acoustic

is generally small, so these two items can be omitted in the analysis.

Assuming that the number of axial rotor segments is n, and the angle of the inclined pole is α, the angle of stagger between each rotor segment is α/(n-1). Neglecting the current time harmonics generated by the PWM modulation, the magnetic potential f_v, f_u expressions of the stator and rotor after the rotor segmentation with inclined poles are equation (2).

$$\begin{cases} f_v = \sum_v F_v \cos(v p\theta - \omega_1 t - \varphi_v) \\ f_\mu = \frac{1}{n} \sum_{m=-(n-1)/2}^{(n-1)/2} \sum_\mu F_\mu \cos\left(\mu p\theta - \omega_\mu t - \varphi_\mu - \mu\alpha \frac{m}{n-1}\right) \end{cases} \tag{2}$$

In order to simplify the analysis and ignore the effect of the inclined pole on the air gap permeability, the air gap permeability per unit area can be used by the equation (3):

$$\begin{cases} \Lambda(\theta,t) = \Lambda_0 + \sum \lambda_{11} \\ \Lambda_0 = \frac{\mu_0}{k_\delta \delta} \\ \lambda_{11} = \Lambda_{l1} \cos(l_1 Z_1 \theta) \\ \Lambda_{l1} = \frac{\mu_0 (k_\delta - 1)}{k_\delta \delta} \left| \frac{\sin\left(l_1 \frac{k_\delta - 1}{k_\delta} \pi\right)}{l_1 \frac{k_\delta - 1}{k_\delta} \pi} \right| \end{cases} \tag{3}$$

Where $\Lambda 0$ is the invariant portion of air gap permeability per unit area, λ_{11} is the harmonic ratio permeability of the stator slotting caused by the periodic component of the permeability, μ_0 is the vacuum permeability, k_δ is the air gap coefficient, δ is the length of the air gap, and Z_1 is the number of stator slots.

Multiply the stator and rotor air-gap magnetic potential expressions (2) with the air-gap permeability expression (3) to obtain the stator and rotor flux density expressions (4) after the rotor is segmented into inclined poles[7]:

$$\begin{aligned} B_v &= \sum_v F_v \Lambda_0 \cos(v p\theta - \omega_1 t - \varphi_v) \\ &\quad + \sum_v \sum_k \frac{F_v \Lambda_k}{2} \cos(v p\theta \pm kZ\theta - \omega_1 t - \varphi_v) \\ B_\mu &= \frac{1}{n} \sum_{m=-(n-1)/2}^{(n-1)/2} \begin{bmatrix} \sum_\mu F_\mu \Lambda_0 \cos(\mu p\theta - \omega_\mu t - \\ \varphi_\mu - \mu\alpha \frac{m}{n-1}) \\ + \sum_\mu \sum_k \frac{F_\mu \Lambda_k}{2} \cos(\mu p\theta \pm kZ\theta \\ -\omega_\mu t - \varphi_\mu - \mu\alpha \frac{m}{n-1}) \end{bmatrix} \end{aligned} \tag{4}$$

The average value of radial EMF wave after rotor segmented inclined pole can be obtained by iterative averaging of EMF wave of each segment, and the average value of radial EMF wave after rotor segmented inclined pole can be obtained according to equations (1) and (4). As in equation (5):

$$\begin{aligned} p_{eq} &= \frac{1}{n} \sum_{m=-(n-1)/2}^{(n-1)/2} \sum_r P_r \cos\left[r\theta - \omega_r t - \varphi_r - \mu\alpha \frac{m}{n-1}\right] \\ &= \frac{1}{n} \sum_r P_r \cos(r\theta - \omega_r t - \varphi_r) \sum_{m=1}^{(n-1)/2} \left[2\cos\left(\mu\alpha \frac{m}{n-1}\right) + 1\right] \\ &= \sum_r P_r k \cos(r\theta - \omega_r t - \varphi_r) \end{aligned} \tag{5}$$

Where: r, ω_r, pr are the order, electrical angle frequency and amplitude of the radial EMF wave, respectively; φ_r is the phase angle; k is the oblique pole coefficient of the rotor segmented oblique pole, the equation is (6):

$$k = \frac{\sin\left(\frac{n}{n-1} \frac{\mu\alpha}{2}\right)}{n \sin\left(\frac{\mu\alpha}{2(n-1)}\right)} \tag{6}$$

The rotor segmented inclined pole can effectively weaken the tooth harmonics, and the weakened tooth harmonic order is closely related to the number of segments. The relationship between the rotor field harmonic number and the tooth harmonic order i is as equation (7):

$$\mu = \frac{\mathrm{LCM}[Z, 2p]}{p} i \pm 1 \tag{7}$$

Where: LCM is the least common multiple function.

In order to achieve the purpose of weakening a certain order of tooth harmonics, the relationship[8] between the optimal skewed pole electrical angle and the order of tooth harmonics can be derived from Eq. (6), as in equation (8):

$$\alpha_{opt} = \frac{2p\pi}{i\mathrm{LCM}(Z, 2p)} \frac{n-1}{n} \tag{8}$$

Combined with (7) and (8), and by making i/n=t, it can be obtained (9):

$$k = \left| \frac{\sin i\pi}{n \sin(i\pi / n)} \right| = \left| \frac{\sin(nt\pi)}{n \sin(t\pi)} \right| \approx \begin{cases} 1, & t \in \mathbf{Z} \\ 0, & t \notin \mathbf{Z} \end{cases} \tag{9}$$

From the above analysis, it can be seen that: when the order of the tooth harmonics is an integer multiple of the number of segments, the rotor inclined pole cannot weaken the order of the tooth harmonics; when it is a non-integer multiple of the order of the tooth harmonics can be effectively suppressed.

2.2 Vibro-acoustic analysis

When the frequency of the r-order excitation force wave is close to the intrinsic frequency of the r-order vibration mode of the motor stator, resonance occurs, which causes high electromagnetic noise. Therefore, the resonance frequency of the motor should be kept away from the frequency of the main excitation force wave, i.e., the low-order excitation force wave, to avoid the occurrence of resonance when the design of the

permanent magnet motor is carried out. The stiffness and mass of the stator core and case of a permanent magnet motor are equation (10):

$$\begin{cases} K_i = \dfrac{2\pi E_i J_i}{R_i^3}\left(r^2-1\right)^2 F_{ri}^2 \\ m_i = G_i \dfrac{r^2+1}{r^2} \\ J_i = \dfrac{h_i^3 l_i}{12} \end{cases} \tag{10}$$

Where: the subscript i = 1,2 represents the core and case, respectively; K_1, K_2 is the stiffness of the core and case; m_1, m_2 is the equivalent mass of the core and case; J_1, J_2 is the inertia of the core and case; G_1 is the total mass of the core yoke, teeth, and windings; G_2 is the mass of the case; R_1, R_2, h_1, h_2, l_1, l_2 is the average radius, yoke thickness, and axial length of the core and case, respectively; E_1, E_2 are the modulus of elasticity of the core and housing, respectively.

Let the amplitude of the r-order excitation force wave acting on the inner surface of the stator armature be P_r, then the equivalent concentrated force is equation (11):

$$P_{\mathrm{re}} = 2\pi R_{\mathrm{i}} l_1 P_r \tag{11}$$

Where R_{i} is the inner radius of the stator core. For the closed permanent magnet motor, set the core and casing without relative tangential displacement, the casing and core vibration and amplitude is equal, the two vibration similar to the same rigid body circle, its stiffness and mass are equal to the casing and the core of the stiffness of the sum and the mass of the sum, then according to the theory of mechanical impedance, vibration displacement is equation (12):

$$Y_{\mathrm{r}} = \frac{P_{\mathrm{re}}}{(K_1+K_2)-\omega_r^2(m_1+m_2)} \tag{12}$$

where ω_r is the angular frequency of r order force wave vibration. Considering the permanent magnet motor as a finite-length cylindrical radiator to calculate the electromagnetic noise generated by the motor, the sound power radiated by the permanent magnet motor are equation (13):

$$\begin{cases} S_{\mathrm{p}} = \rho_0 c_0 \left(\dfrac{\omega_{\mathrm{r}} Y_{\mathrm{r}}}{\sqrt{2}}\right)^2 S_{\mathrm{f}} \\ S_{\mathrm{PL}} = 10\lg\left(\dfrac{S_{\mathrm{p}}}{10^{-12}}\right) \\ S_{\mathrm{PLre}} = 10\log\left(\sum 10^{\frac{S_{\mathrm{PL}i}}{10}}\right) \end{cases} \tag{13}$$

where: ρ_0 is the density of air; c_0 is the propagation speed of sound waves in air; S_f is the surface area of the acoustic radiation model of the motor. S_{PL} is the sound power level, S_{PLre} is the synthesized sound power level.

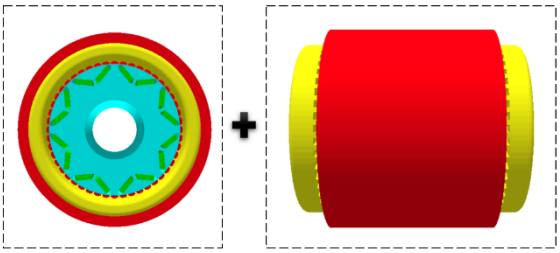

Fig. 1 Prototype motor model.

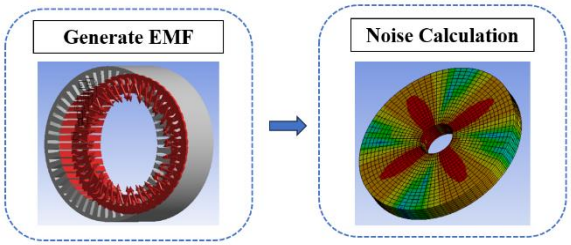

Fig. 2 Vibro-acoustic Calculation Flow.

Table 1. Basic parameters of the prototype motor

Poles	8	Inner diameter of stator	140mm
Slots	48	Iron core stack length	110mm
Magnetic pole type	V	Inner diameter of rotor	78mm
Outer diameter of stator	210mm	Outer diameter of rotor	138.6mm

The above formulas can be quickly analyzed and calculated for vibro-acoustic, and complex multi-physical field coupling can be calculated with the help of FEA.

3 Analysis Prototypes under MOC through FEA

In Chapter II, the formulae for the EMF on the rotor under skewed poles are given, as well as the formulae for the vibration and noise of the motor under EMF. In this chapter, for an 8-pole 48-slot motor, the vibration and noise under multiple working conditions are simulated, and the order and frequency of the vibration and noise are analyzed, based on the results of the simulation combined with the theory in Chapter II. The prototype motor is shown in Fig. 1. The motor parameters are shown in Table 1.

3.1 Vibro-acoustic Analysis by FEA under skewed pole

This subsection presents the vibro-acoustic simulation for the 8-pole 48-slot motor. The EMF mainly acts on the teeth of the stator, which is transmitted through the stator teeth to the stator yoke and radiates noise outward. In this subsection, the harmonic EMF is first calculated by ANSYS Maxwell under MOC, and then the EMF is applied to the stator teeth in the

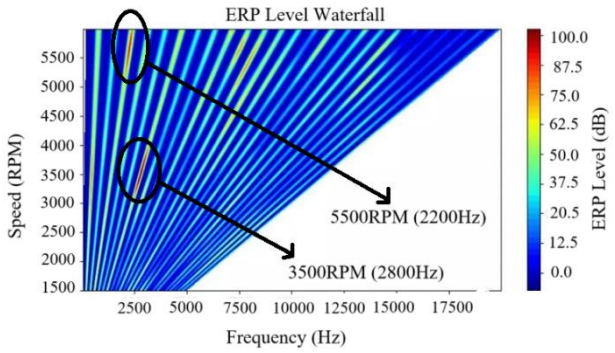

Fig. 3 ERPL waterfall.

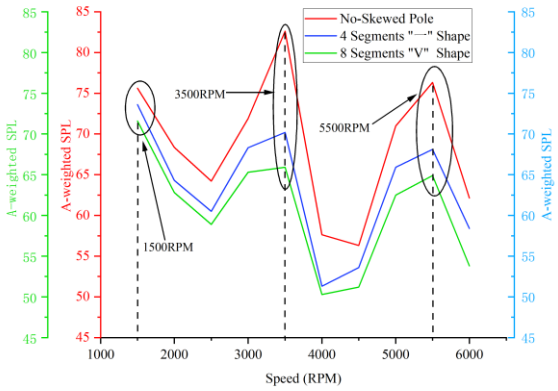

Fig. 4 A-weighted SPL at multiple rotational speeds.

Table 2. Types of skewed poles

Skewed Pole Type	No-Skewed Pole	4-Segments Continuous Skewed	8-Segments V-Shape Skewed
Geometry			

Table 3. Skewed pole angle

	Angle of skewed pole of each segment							
Skewed Pole Type	1	2	3	4	5	6	7	8
No-Skewed Pole	0	0	0	0	0	0	0	0
4-Segments Continuous Skewed	-2.8	-0.9	0.9	2.8	-	-	-	-
8-Segments V-Shape Skewed	-2.8	-0.9	0.9	2.8	2.8	0.9	-0.9	-2.8

Table 4. Comparison of optimization effect under different inclined pole types

Skewed Pole Type	3500 RPM	Optimization effect	5500 RPM	Optimization effect
No-Skewed Pole	82.59 dB		77.8 dB	
4-Segments Continuous Skewed	69.3 dB	16.1%↑	67.9 dB	12.7%↑
8-Segments V-Shape Skewed	66.3 dB	19.7%↑	64.1 dB	17.6%↑

ANSYS harmonic response module to calculate the vibration of the stator yoke, and the vibration data under MOC are imported to the harmonic acoustics module for the calculation of acoustic. The vibro-acoustic calculation process is shown in Fig. 2.

The vibro-acoustic ERPL waterfall of the prototype motor at 1500RPM-6000RPM operating conditions is shown in Fig. 3. It can be seen that 5500rpm-2200Hz, 3500rpm-2800Hz at the ERPL value is larger, according to the theoretical analysis of the motor in Chapter II, it can be seen that the former is the stator 5th, 7th the harmonics and rotor the same number of times of the interaction of the harmonics of the permanent magnet magnetic field, the two spatial poles are equal to the number of pairs of synthesized force wave poles of 0, which will cause a larger amplitude, the use of the Short pitch winding and rotor pole repair can be weakened; the latter is the stator armature reaction fundamental wave potential generated by the 11th and 13th tooth harmonics and rotor permanent magnet magnetic field of the 11th and 13th tooth harmonics generated by the interaction of the two spatial poles are equal to the number of pairs of synthetic force wave poles are also 0, the same caused by a large amplitude, generally using a continuous skewed pole or skewed groove can be basically eliminated by the axial 0th-order EMF caused by the tooth harmonics components.

3.2 Vibro-acoustic optimization

Considering that the basic electromagnetic parameters and dimensions of the 8-pole 48-slot prototype motor have been determined, this paper adopts the vibration damping measure of rotor segmented inclined poles to optimize the vibration acoustics at these two frequency points, and the commonly used skewed poles are the Continuous skewed pole and the V-pole skewed pole, and the vibration damping and noise reduction effects of the non-used inclined poles are different. The skewed pole type used in this paper and the angle of the skewed pole are shown in Tables II and III. In this paper, the A-weighted SPL of the motor at 1500RPM-6000RPM with different types of inclined poles is calculated using finite element analysis as shown in Fig. 4. By comparing the A-weighted SPL results at full speed, it is found that the noise reduction effect of adopting 8-section V-type inclined pole is better, and the noise is larger at 3500RPM and 5500RPM, and its noise reduction comparison effect is shown in Table IV. It

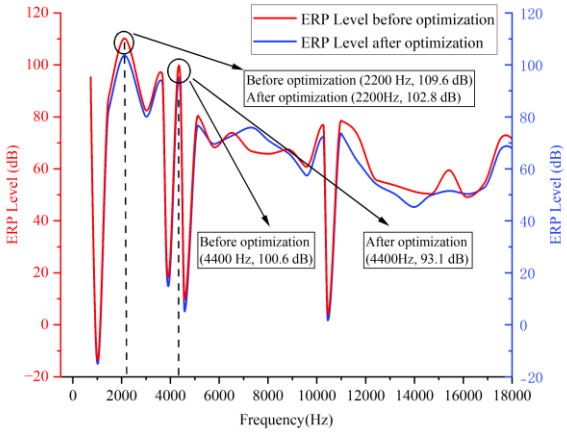

Fig. 5 ERPL waterfall at 5500RPM.

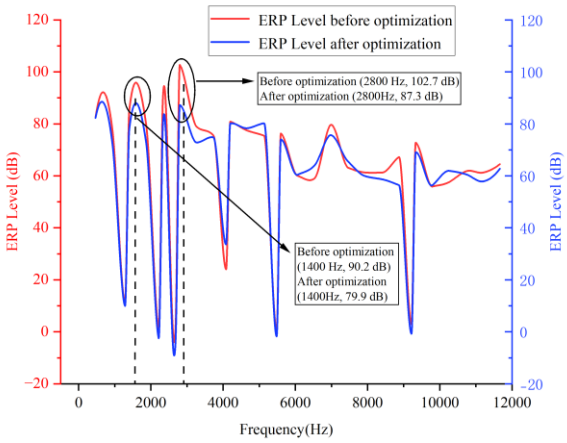

Fig. 6 ERPL waterfall at 3500RPM.

can be seen that the noise of the motor with V-type skewed poles is 10% and 15% lower than that of the motor without skewed poles at 3500RPM and 5500RPM, respectively; the noise of the motor with continuous skewed poles is 8% and 9% lower than that of the motor without skewed poles at 3500RPM and 5500RPM, respectively.

After the rotor adopts 8-segment V-type skewed poles, the ERPLs at each frequency point before and after optimization are shown in Figs. 5 and 6 for the two working conditions of 5500RPM and 3500RPM. The ERPL data before and after optimization for 5500RPM-2200Hz/4400Hz and 3500RPM-2800Hz/1400Hz are shown in Table V and Table VI. It can be seen that after optimization, at 5500RPM, the vibration optimization effect of 2200Hz and 4400Hz is improved by 6.2% and 7.4% respectively; at 3500RPM, the vibration optimization of 1400Hz and 2800Hz is improved by 11.4% and 14.9% respectively.

Through the analysis of the above optimization data, it can be seen that the rotor inclined pole can significantly reduce the

Table 5. Vibro-acoustic optimization at 5500RPM

	5500RPM-2200Hz	5500RPM-4400Hz
Before optimization	109.6 dB	100.6 dB
After optimization	102.8 dB	93.1 dB
Optimization effect	6.2%↑	7.4%↑

Table 6. Vibro-acoustic optimization at 3500RPM.

	3500RPM-1400Hz	3500RPM-2800Hz
Before optimization	90.2 dB	102.7 dB
After optimization	79.9 dB	87.3 dB
Optimization effect	11.4%↑	14.9%↑

harmonic electromagnetic field amplitude, which in turn reduces the vibration sound. In summary, the rotor V-type inclined pole is an effective means of vibration and noise reduction, under the premise of ensuring the electromagnetic performance and mechanical strength performance, the reasonable design of the inclined pole method can effectively reduce the vibration sound of the motor under the MOC.

4 Conclusion

In this paper, a comprehensive optimization of the vibro-acoustics of IPMSM is accomplished by adopting an 8-segment V-shaped skewed pole by the rotor with the objective of weakening the harmonic electromagnetic field. The conclusions are as follows:

The vibro-acoustic simulation of the prototype motor at full speed is carried out by FEA, and the equivalent radiation waterfall diagram shows that the motor vibro-acoustic is larger at the two points of 3500RPM-2800Hz,5500RPM-2200Hz, which is generated by the interaction of the stator's first-order tooth harmonics in combination with the theoretical analysis of the motor electromagnetism and the interaction of the stator's 5th and 7th harmonics in the latter case. The rotor can suppress the tooth harmonics by adopting the oblique pole, comparing the A-weighted SPL data under the two oblique pole modes of 4-section continuous oblique pole and 8-section V-type oblique pole, it can be seen that the 8-section V-type oblique pole has a better effect on suppressing the tooth harmonics, and the total vibro-acoustic is reduced by 22.5%.

The limitations of this study are threefold: the validation dimension relies on finite element simulation (FEA) without experimental bench validation; the working condition coverage is is limited to the speed range of 1500-6000 RPM and lacks the analysis of extreme temperature/load fluctuations; the topology exploration is limited to the continuous inclined pole and V-type inclined pole The topology exploration is limited to continuous and V-shaped inclined pole, and other structures such as helical inclined pole are not evaluated. In order to make up for the shortcomings, future work suggests: deepen the experimental validation, develop intelligent optimization model For example,

combining machine learning algorithms to globally optimize the helical pole parameters, and expanding the application of new materials, such as exploring the synergistic design of soft magnetic composites and helical pole rotors to suppress high-frequency noise.

5 References

[1] D. Wang, X. Wang, B. Wang, J. Nie, J. Li and X. Wang, "Dynamic Eccentricity Impact on Electromagnetic Vibration and Acoustic Noise of Interior Permanent Magnet Synchronous Motors With Different Numbers of Parallel Branches," in IEEE Transactions on Transportation Electrification, vol. 11, no. 1, pp. 3337-3348, Feb. 2025.

[2] Q. Li, S. Liu and Y. Hu, "Vibration Characteristics of Permanent Magnet Motor Stator System Based on Vibro-Inertance Matrix Method," in IEEE Transactions on Energy Conversion, vol. 37, no. 3, pp. 1777-1788, Sept. 2022.

[3] Q. Chen et al., "Analysis of Electromagnetic Noise Mechanism in Internal/External Rotor Axial-Flux Motors Considering Magnetic Field Modulation Effect," in IEEE Transactions on Transportation Electrification, vol. 11, no. 1, pp. 2391-2404, Feb. 2025.

[4] H. Zhuang, S. Zuo, Z. Ma, B. Yin and C. Liu, "Novel Effective Torque Analysis Method for Interior Permanent Magnet Synchronous Machines," in IEEE Transactions on Transportation Electrification, vol. 11, no. 1, pp. 4202-4213, Feb. 2025.

[5] D. Li, Y. Xie, W. Cai, F. Zhang and Y. Sun, "An Analytical Prediction Method for Zero-Order Vibration and Noise of Permanent Magnet Synchronous Motor," in IEEE Transactions on Applied Superconductivity, vol. 34, no. 8, pp. 1-6, Nov. 2024

[6] Q. Li, S. Liu, X. Li and Y. Hu, "Vibro-Inertance Matrix Supported OCF Characteristics Analysis of PMSM Under Multiple Operating Conditions for EV," in IEEE Transactions on Industrial Electronics, vol. 71, no. 1, pp. 126-137, Jan. 2024.

[7] D. Li, Y. Xie, W. Cai and F. Zhang, "Vibration Mitigation of Interior Permanent Magnet Synchronous Motor Using a Targeted Rotor-Step Skewing Method," in IEEE Transactions on Transportation Electrification, vol. 11, no. 1, pp. 2160-2170, Feb. 2025.

[8] C. Peng, D. Wang, B. Wang, J. Li, C. Wang and X. Wang, "Different Rotor Segmented Approaches for Electromagnetic Vibration and Acoustic Noise Mitigation in Permanent Magnet Drive Motor: A Comparative Study," in IEEE Transactions on Industrial Electronics, vol. 71, no. 2, pp. 1223-1233, Feb. 2024.

[9] Y. Zhou, X. Wei, L. Yan and X. He, "Hybrid Analytical-Numerical Electromagnetic Vibration Calculation Method for Surface-Inserted PMSMs With Skewed Slots," in IEEE Transactions on Energy Conversion, vol. 39, no. 4, pp. 2654-2663, Dec. 2024.